Electromagnetic-Compliant Channel Modeling and Performance Evaluation for Holographic MIMO

Tengjiao Wang*, Wei Han*, Zhimeng Zhong*, Jiyong Pang*, Guohua Zhou*, Shaobo Wang*, Qiang Li†

2022.12.4

*Wireless Network RAN Research Department, Huawei Technologies CO., Ltd, Shanghai, China

†Department of Broadband Communication, Peng Cheng Laboratory, Shenzhen, China

Background

- **Holographic MIMO**: By integrating an infinite number of antennas into a limited surface, holographic MIMO is expected to fully exploit the propagation characteristics offered by the electromagnetic channel and approach the fundamental performance limit. [3-4]

- **EM-Compliant Channel Modeling**: One of the key challenges for Holographic MIMO. [8-10]

- **Key Problems**: Non-isotropic scattering, non-ideal factors including the distortion of antenna patterns and the decrease of antenna efficiency are not taken into consideration in the state-of-the-art channel models. [11-12]

Contributions

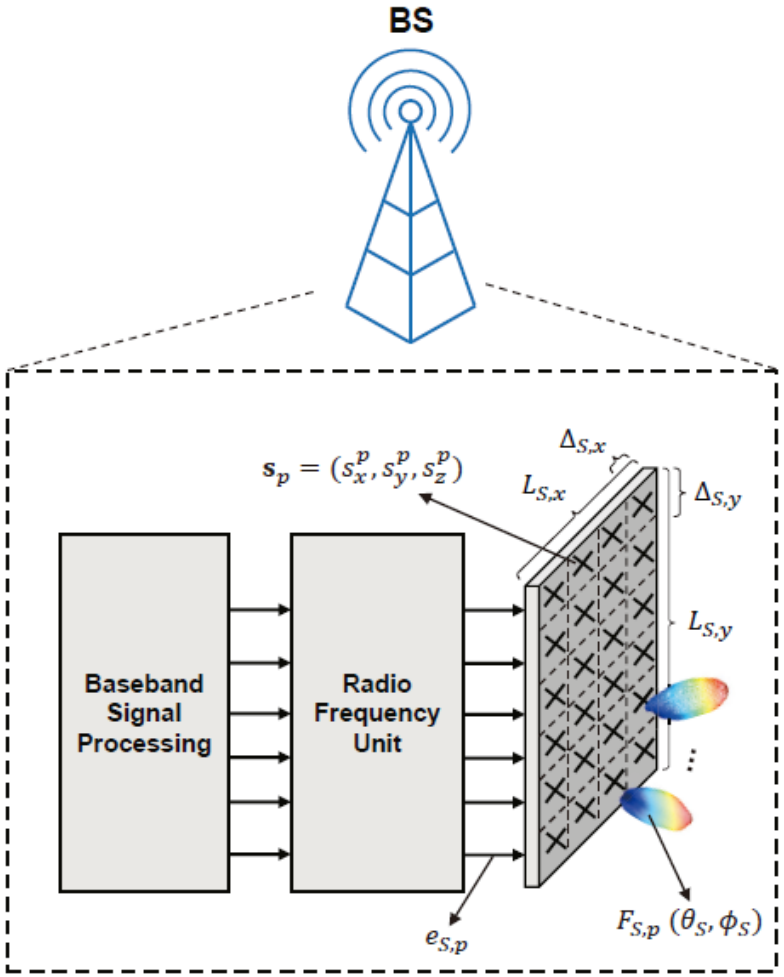
- An **EM-compliant channel model** is proposed for the holographic MIMO systems. Based on the von Mises-Fisher (VMF) distributions [13] and the 3GPP TR 38.901 channel model [14], a **realistic angular power spectrum** is modeled, which has intuitive physical meaning and is more consistent with the realistic environment.

- The **non-ideal factors** caused by antenna mutual coupling at the transceivers are taken into consideration, including the **antenna pattern distortion** and the **decrease of antenna efficiency**.

- Using the proposed channel model, a more realistic **performance evaluation** is conducted in both the single-user and multi-user scenarios. Simulation results are provided to show the performance and **technical challenges** for the future holographic MIMO systems.

Fourier Plane-Wave Series Expansion-Based Channel Model [8]–[10]

We consider a holographic MIMO system equipped with uniform planar arrays at both the base station (BS) and the user equipment (UE).



Channel matrix

$$\mathbf{H} = \sqrt{N_{\mathrm{R}} N_{\mathrm{S}}} \times \sum_{l_x, l_y} \sum_{m_x, m_y} H_{\mathrm{a}}(l_x, l_y, m_x, m_y) \mathbf{a}_{\mathrm{R}}(l_x, l_y) \mathbf{a}_{\mathrm{S}}^{\mathrm{H}}(m_x, m_y),$$

Phase-shifted 2D Fourier harmonics

$$[\mathbf{a}_{\mathrm{S}}(m_x, m_y)]_p = \frac{1}{\sqrt{N_{\mathrm{S}}}} e^{-j\left(\frac{2\pi m_x}{L_{\mathrm{S},x}} s_x^p + \frac{2\pi m_y}{L_{\mathrm{S},y}} s_y^p + \gamma_{\mathrm{S}}(m_x, m_y) s_z^p\right)},$$

$$[\mathbf{a}_{\mathrm{R}}(l_x, l_y)]_q = \frac{1}{\sqrt{N_{\mathrm{R}}}} e^{j\left(\frac{2\pi l_x}{L_{\mathrm{R},x}} r_x^q + \frac{2\pi l_y}{L_{\mathrm{R},y}} r_y^q + \gamma_{\mathrm{R}}(l_x, l_y) r_z^q\right)}$$

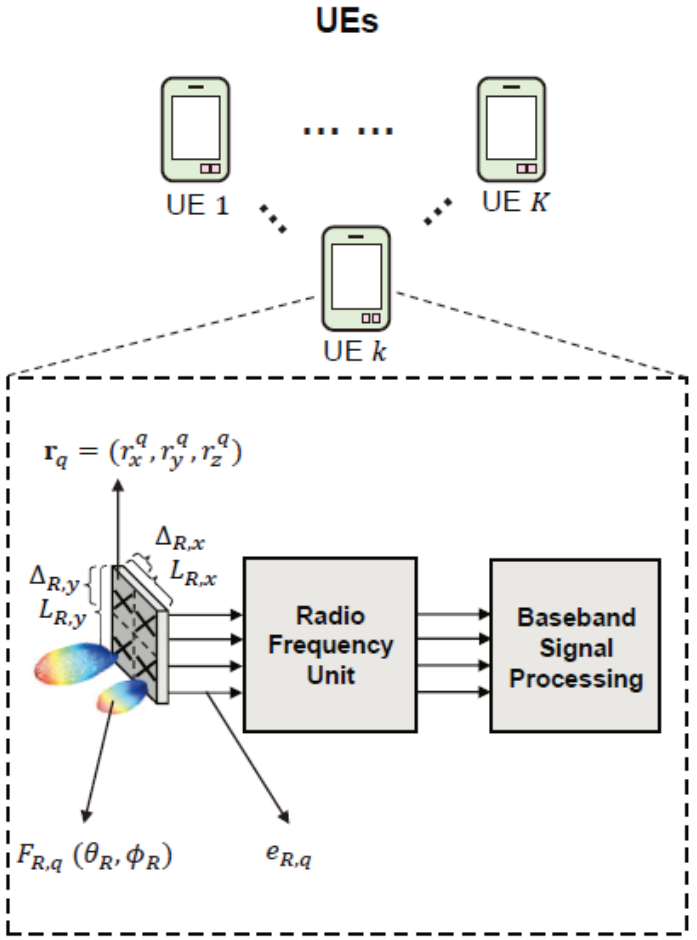
Random Fourier coefficient

$$H_{\mathrm{a}}(l_x, l_y, m_x, m_y) \sim \mathcal{CN}(\sigma^2(l_x, l_y, m_x, m_y))$$

$$\sigma^2(l_x, l_y, m_x, m_y) = \iint_{\Omega_{\mathrm{R}}(l_x, l_y)} A^2(\theta_{\mathrm{R}}, \phi_{\mathrm{R}}) \sin\theta_{\mathrm{R}} \mathrm{d}\theta_{\mathrm{R}} \mathrm{d}\phi_{\mathrm{R}} \times \iint_{\Omega_{\mathrm{S}}(m_x, m_y)} A^2(\theta_{\mathrm{S}}, \phi_{\mathrm{S}}) \sin\theta_{\mathrm{S}} \mathrm{d}\theta_{\mathrm{S}} \mathrm{d}\phi_{\mathrm{S}},$$

Final Channel matrix

$$\mathbf{H} = \mathbf{U}_{\mathrm{R}} \mathbf{H}_{\mathrm{a}} \mathbf{U}_{\mathrm{S}}^{\mathrm{H}}$$



Proposed EM-Compliant Channel Model - Overall

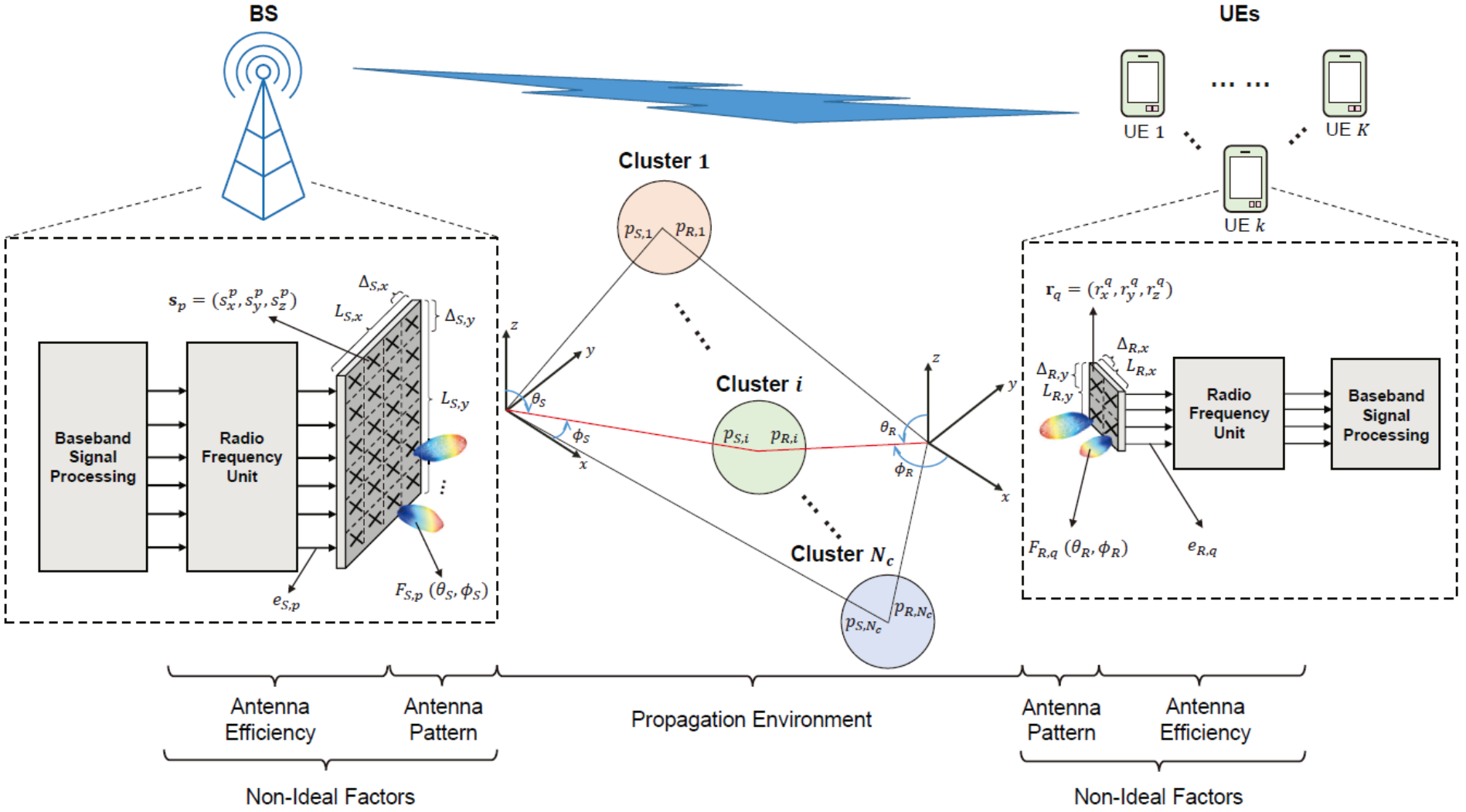


Fig. 1. Illustration of the proposed EM-compliant channel model for holographic MIMO systems, including the characteristics of the propagation environment and the non-ideal factors at the transceivers.

Proposed EM-Compliant Channel Model – Angular Power Spectrum

Mises-Fisher (VMF) distributions [13]

3GPP TR 38.901 [14]

Angular power spectrum

$$A_{\mathrm{S}}^2(\theta_{\mathrm{S}},\phi_{\mathrm{S}}) = \sum_{i=1}^{N_c} w_{\mathrm{S},i} p_{\mathrm{S},i}(\theta_{\mathrm{S}},\phi_{\mathrm{S}})$$

$$A_{\mathrm{R}}^2(\theta_{\mathrm{R}},\phi_{\mathrm{R}}) = \sum_{i=1}^{N_c} w_{\mathrm{R},i} p_{\mathrm{R},i}(\theta_{\mathrm{R}},\phi_{\mathrm{R}})$$

PDF of 3D VMF distribution

$$p_{\mathrm{S},i}(\theta_{\mathrm{S}},\phi_{\mathrm{S}}) = \frac{\alpha_{\mathrm{S},i}}{4\pi \sinh(\alpha_{\mathrm{S},i})} \times e^{\alpha_{\mathrm{S},i}(\sin\theta_{\mathrm{S}} \sin\bar{\theta}_{\mathrm{S},i} \cos(\phi_{\mathrm{S}}-\bar{\phi}_{\mathrm{S},i})+\cos\theta_{\mathrm{S}} \cos\bar{\theta}_{\mathrm{S},i})}$$

$$p_{\mathrm{R},i}(\theta_{\mathrm{R}},\phi_{\mathrm{R}}) = \frac{\alpha_{\mathrm{R},i}}{4\pi \sinh(\alpha_{\mathrm{R},i})} \times e^{\alpha_{\mathrm{R},i}(\sin\theta_{\mathrm{R}} \sin\bar{\theta}_{\mathrm{R},i} \cos(\phi_{\mathrm{R}}-\bar{\phi}_{\mathrm{R},i})+\cos\theta_{\mathrm{R}} \cos\bar{\theta}_{\mathrm{R},i})}$$

Normalization factor

$$\sum_i^{N_c} w_{\mathrm{S},i} = \sum_i^{N_c} w_{\mathrm{R},i} = 1$$

Cluster delay line (CDL)

$$\bar{\phi}_{\mathrm{S},i} = \phi_{i,\mathrm{AoD}} \quad \bar{\theta}_{\mathrm{S},i} = \theta_{i,\mathrm{ZoD}}$$

$$\bar{\phi}_{\mathrm{R},i} = \phi_{i,\mathrm{AoA}} \quad \bar{\theta}_{\mathrm{R},i} = \theta_{i,\mathrm{ZoA}}$$

*Table 7.7.1-2 in [14]

Concentration parameter

$$\alpha_{\mathrm{S},i} = \frac{212.9^2}{\delta_{\mathrm{ASD}}^2}, \quad \alpha_{\mathrm{R},i} = \frac{212.9^2}{\delta_{\mathrm{ASA}}^2}$$

*Appendix 3.1 in [15]

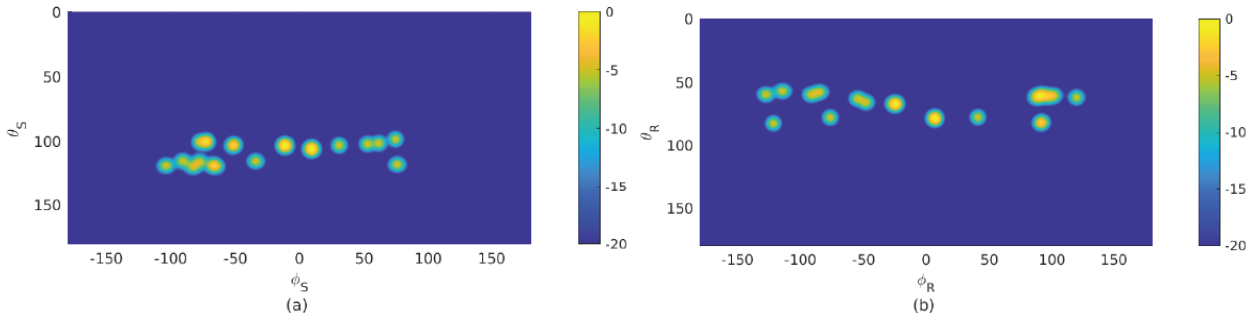


Fig. 2. Illustration of the anglular power spectrum of the propagation channel based on 3GPP CDL-B channel model. a) Anglular power spectrum at BS; b) Anglular power spectrum at UE..

Proposed EM-Compliant Channel Model – Antenna Pattern Distortion

- Firstly, the **distorted antenna pattern** will be different from that of an **isolated element**.
- Secondly, the distorted antenna patterns of **different elements** will also be different based on the **locations** of the elements in the array

Normalized embedded antenna pattern

$$F_{\mathrm{S},p}(\theta_{\mathrm{S}},\phi_{\mathrm{S}}) \qquad F_{\mathrm{R},q}(\theta_{\mathrm{R}},\phi_{\mathrm{R}})$$

Modified Fourier harmonic

$$[\boldsymbol{\psi}_{\mathrm{S}}(m_x,m_y)]_p = \frac{1}{\sqrt{N_{\mathrm{S}}}} e^{-j\left(\frac{2\pi m_x}{L_{\mathrm{S},x}} s_x^p + \frac{2\pi m_y}{L_{\mathrm{S},y}} s_y^p + \gamma_{\mathrm{S}}(m_x,m_y) s_z^p\right)} \times F_{\mathrm{S},p}\left(\theta_{\mathrm{S}}^*(m_x,m_y), \phi_{\mathrm{S}}^*(m_x,m_y)\right),$$

$$[\boldsymbol{\psi}_{\mathrm{R}}(l_x,l_y)]_q = \frac{1}{\sqrt{N_{\mathrm{R}}}} e^{j\left(\frac{2\pi l_x}{L_{\mathrm{R},x}} r_x^q + \frac{2\pi l_y}{L_{\mathrm{R},y}} r_y^q + \gamma_{\mathrm{R}}(l_x,l_y) r_z^q\right)} \times F_{\mathrm{R},q}\left(\theta_{\mathrm{R}}^*(l_x,l_y), \phi_{\mathrm{R}}^*(l_x,l_y)\right),$$

Elevation angle

$$\theta_{\mathrm{S}}^*(m_x,m_y) = \arccos\left(\sqrt{1-\left(\frac{m_x\lambda}{L_{\mathrm{S},x}}\right)^2 - \left(\frac{m_y\lambda}{L_{\mathrm{S},y}}\right)^2}\right)$$

$$\theta_{\mathrm{R}}^*(l_x,l_y) = \arccos\left(\sqrt{1-\left(\frac{l_x\lambda}{L_{\mathrm{R},x}}\right)^2 - \left(\frac{l_y\lambda}{L_{\mathrm{R},y}}\right)^2}\right)$$

Azimuth angle

$$\phi_{\mathrm{S}}^*(m_x,m_y) = \arctan\left(\frac{L_{\mathrm{S},x} m_y}{L_{\mathrm{S},y} m_x}\right)$$

$$\phi_{\mathrm{R}}^*(l_x,l_y) = \arctan\left(\frac{L_{\mathrm{R},x} l_y}{L_{\mathrm{R},y} l_x}\right)$$

Over Channel Matrix

$$\mathbf{H} = \boldsymbol{\Psi}_{\mathrm{R}} \mathbf{H}_{\mathrm{a}} \boldsymbol{\Psi}_{\mathrm{S}}^{\mathrm{H}}$$

Proposed EM-Compliant Channel Model – Antenna Efficiency

- In a dense antenna array with small element spacing, the efficiency of the antenna elements will be decreased because of the **mutual coupling** among them.
- The reason is that due to the effect of **mutual coupling**, the **active impedance** of each element varies with **scan angles**. The **impedance mismatch** between the antenna elements and the transmission lines causes the power to be returned to the generators.

Antenna Efficiency

$$e_{\mathrm{S},p} = 1 - \sum_{p'=1}^{N_\mathrm{S}} \|[\mathbf{S}_\mathrm{S}]_{p,p'}\|^2,$$

$$e_{\mathrm{R},q} = 1 - \sum_{q'=1}^{N_\mathrm{R}} \|[\mathbf{S}_\mathrm{R}]_{q,q'}\|^2,$$

Hannan's Efficiency [16]

$$e^*_{\mathrm{S},p}(\Delta_{\mathrm{S},x}, \Delta_{\mathrm{S},y}) = \frac{\pi L_{\mathrm{S},x} L_{\mathrm{S},y}}{N_\mathrm{S}\lambda^2} = \frac{\pi \Delta_{\mathrm{S},x} \Delta_{\mathrm{S},y}}{\lambda^2}$$

$$e^*_{\mathrm{R},q}(\Delta_{\mathrm{R},x}, \Delta_{\mathrm{R},y}) = \frac{\pi L_{\mathrm{R},x} L_{\mathrm{R},y}}{N_\mathrm{R}\lambda^2} = \frac{\pi \Delta_{\mathrm{R},x} \Delta_{\mathrm{R},y}}{\lambda^2}$$

Relative Efficiency

$$\eta_{\mathrm{S},p} = \frac{e_{\mathrm{S},p}}{e^*_{\mathrm{S},p}(\frac{\lambda}{2}, \frac{\lambda}{2})}$$

$$\eta_{\mathrm{R},q} = \frac{e_{\mathrm{R},q}}{e^*_{\mathrm{R},q}(\frac{\lambda}{2}, \frac{\lambda}{2})}.$$

Over Channel Matrix

$$\mathbf{H} = \mathbf{\Gamma}_\mathrm{R} \mathbf{\Psi}_\mathrm{R} \mathbf{H}_\mathrm{a} \mathbf{\Psi}_\mathrm{S}^\mathrm{H} \mathbf{\Gamma}_\mathrm{S}$$

Numerical Results – Single-User Scenario

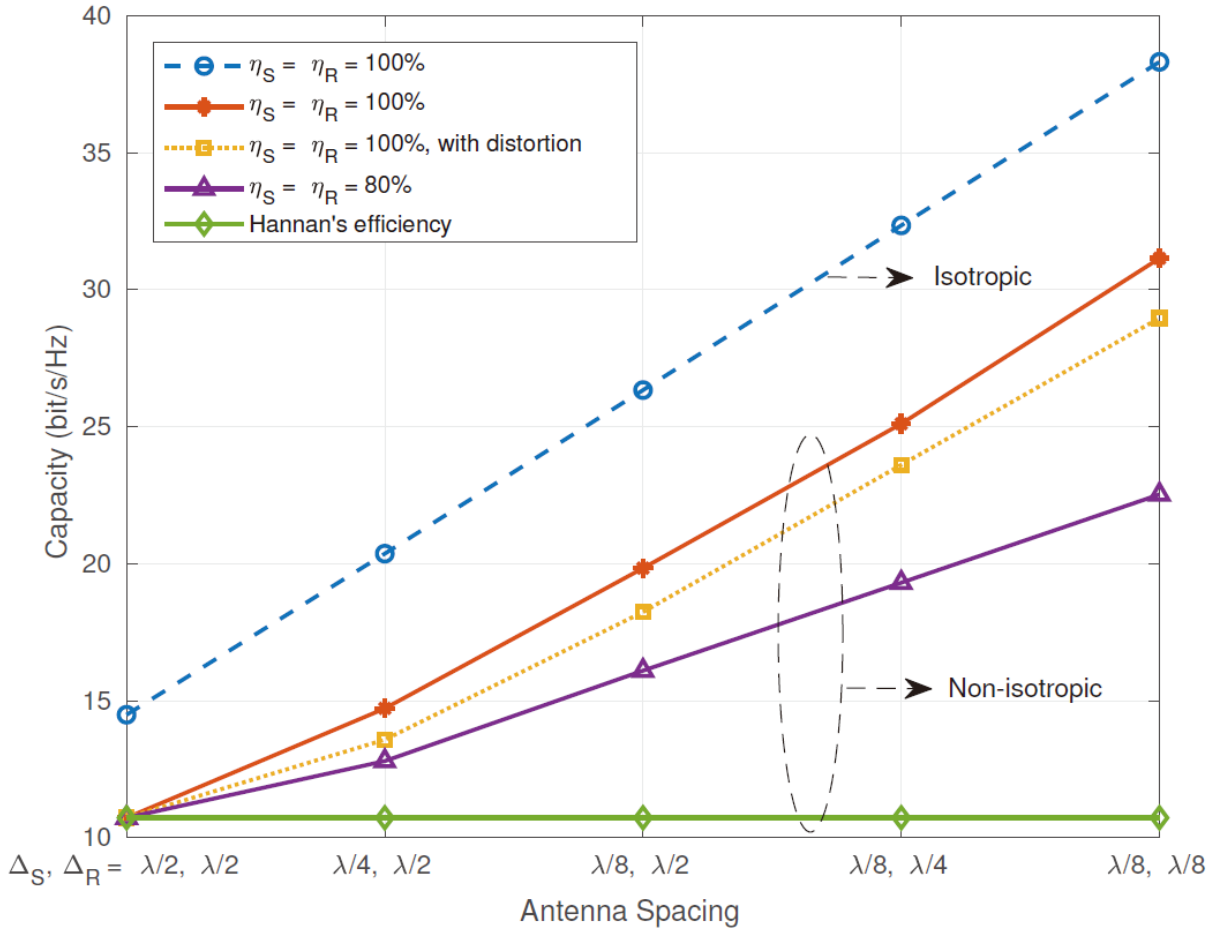


Fig. 3. Ergodic capacity of a single-user holographic MIMO system with different antenna spacing at BS and UE.

Main Findings

- The characteristics of the **scattering environment** affect the channel capacity.
- The **antenna efficiency** has significant impact on the channel capacity of holographic MIMO.
- The **antenna pattern distortion** may also decrease the channel capacity.

- Central frequency: 3.5 GHz
- Size of antenna arrays at BS: $4\lambda \times 4\lambda$
- Size of antenna arrays at UE: $\lambda \times \lambda$
- Non-isotropic: 23 clusters, 3GPP TR 38.901 CDL-B
- SNR = 0 dB
- Power Allocation: water filling

Numerical Results – Multi-User Scenario

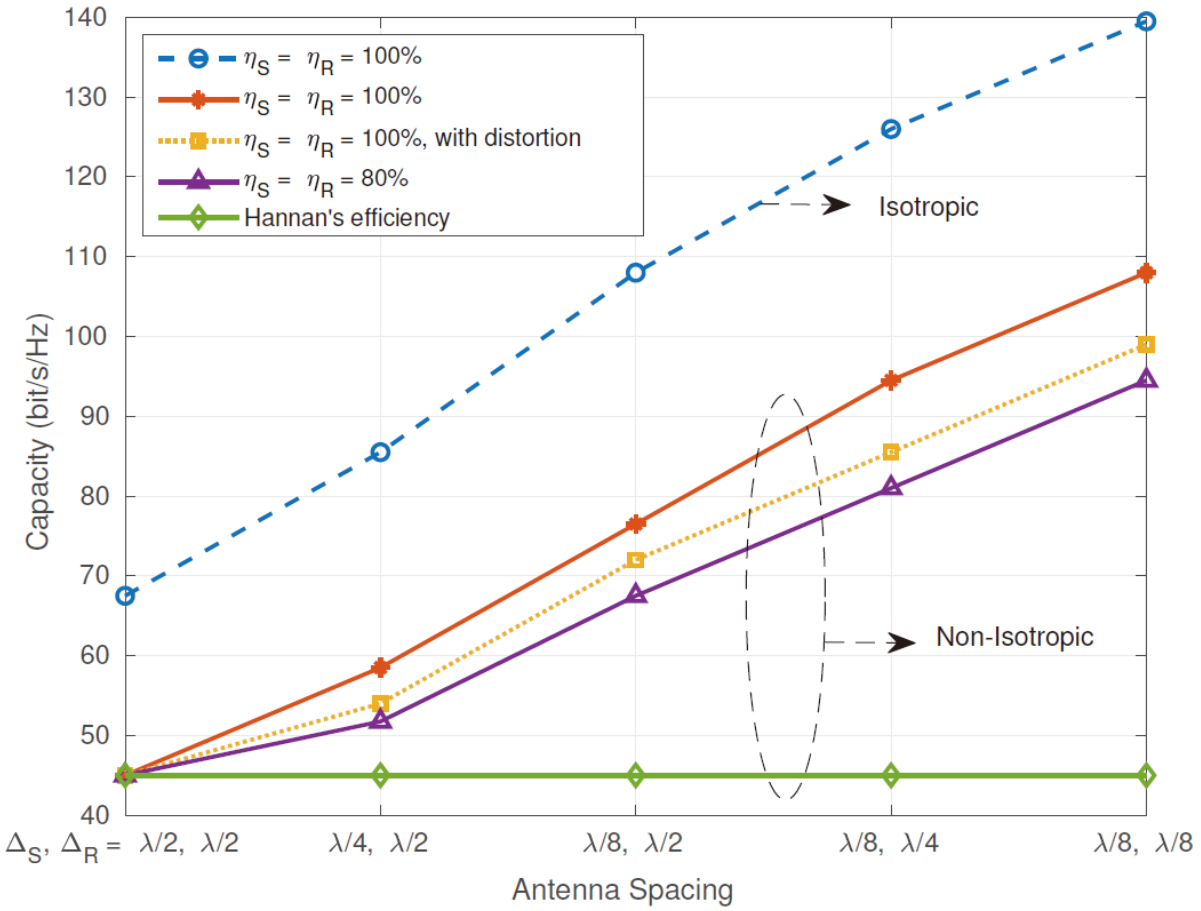


Fig. 4. Ergodic capacity of a multi-user holographic MIMO system with different antenna spacing at BS and UEs.

Similar Findings Can be Found

- **Scattering environment**
- **Antenna efficiency**
- **Antenna pattern distortion**

- Central frequency: 3.5 GHz
- Size of antenna arrays at BS: $4\lambda \times 4\lambda$
- Size of antenna arrays at UE: $\lambda \times \lambda$
- Non-isotropic: 23 clusters, 3GPP TR 38.901 CDL-B
- SNR = 0 dB
- Power Allocation: iterative water filling
- Number of UE: 10
- UE distribution: uniformly distributed in one sector with [120°, -120°], [25m, 100m]
- Large-scale pathloss: UMa in 3GPP TR 38.901

Challenges for Holographic MIMO

- **Antenna Efficiency**: The efficiency of the antenna element is decreased because of mutual coupling and impedance mismatch. Adaptive impedance matching networks and super-gain antennas may be possible ways to increase the element efficiency.

- **Antenna Pattern Distortion**: The distortion of individual antenna patterns has negative impact of the beamforming effect, which affect the overall capacity of the system.

- **Channel Correlation**: The angular power spectrum determines the channel correlation. Smart environment control techniques may be needed to decrease the channel correlation and increase the capacity

Summary

Contributions:

1. An **EM-compliant channel model** is proposed for the holographic MIMO systems which has intuitive physical meaning and is more consistent with the realistic environment.
2. The **non-ideal factors** are taken into consideration, including the **angular power spectrum**, **antenna pattern distortion** and the **decrease of antenna efficiency**.
3. Using the proposed channel model, a more realistic **performance evaluation** is conducted in both the single-user and multi-user scenarios.

Main Findings:

1. The characteristics of the **scattering environment** affect the channel capacity.
2. The **antenna efficiency** has significant impact on the channel capacity of holographic MIMO.
3. The **antenna pattern distortion** may also decrease the channel capacity.

Key Challenges:

1. **Antenna Efficiency**: The efficiency of the antenna element is decreased because of mutual coupling and impedance mismatch.
2. **Antenna Pattern Distortion**: The distortion of individual antenna patterns has negative impact of the beamforming effect, which affect the overall capacity of the system.
3. **Channel Correlation**: The angular power spectrum determines the channel correlation.

Reference

- [1] E. Bjornson, L. Sanguinetti, H. Wymeersch, J. Hoydis, and T. L. Marzetta, "Massive MIMO is a reality-What is next?: Five promising research directions for antenna arrays," *Digit. Signal Process.*, vol. 94, pp. 3–20, Nov. 2019.
- [2] M. Chafii, L. Bariah, S. Muhaidat, and M. Debbah, "Ten scientific challenges for 6G: Rethinking the foundations of communications theory," arXiv, 2022. [Online]. Available: https://arxiv.org/abs/2207.01843
- [3] C. Huang, S. Hu, G. C. Alexandropoulos, A. Zappone, C. Yuen, R. Zhang, M. D. Renzo, and M. Debbah, "Holographic MIMO surfaces for 6G wireless networks: Opportunities, challenges, and trends," *IEEE Wireless Commun.*, vol. 27, no. 5, pp. 118–125, Oct. 2020.
- [4] D. Dardari and N. Decarli, "Holographic communication using intelligent surfaces," *IEEE Commun. Mag.*, vol. 59, no. 6, pp. 35–41, Jun. 2021.
- [5] Z. Zhang and L. Dai, "Continuous-aperture MIMO for electromagnetic information theory," arXiv, 2021. [Online]. Available: https://arxiv.org/abs/2111.08630
- [6] S. S. A. Yuan, Z. He, X. Chen, C. Huang, and W. E. I. Sha, "Electromagnetic effective degree of freedom of an MIMO system in free space," *IEEE Antennas Wireless Propag. Lett.*, vol. 21, no. 3, pp. 446–450, Mar. 2022.
- [7] O. T. Demir, E. Bjornson, and L. Sanguinetti, "Channel modeling and channel estimation for holographic massive MIMO with planar arrays," *IEEE Wireless Commun. Lett.*, vol. 11, no. 5, pp. 997–1001, May 2022.
- [8] A. Pizzo, T. L. Marzetta, and L. Sanguinetti, "Spatially-stationary model for holographic MIMO small-scale fading," *IEEE J. Sel. Areas Commun.*, vol. 38, no. 9, pp. 1964–1979, Sep. 2020.
- [9] L. Wei, C. Huang, G. Alexandropoulus, W. E. Sha, Z. Zhang, M. Debbah, and C. Yuen, "Multi-user holographic MIMO surfaces: Channel modeling and spectral efficiency analysis," IEEE J. Sel. Topics Signal Process., 2022, to be published.

Reference

- [10] A. Pizzo, L. Sanguinetti, and T. L. Marzetta, “Fourier plane-wave series expansion for holographic MIMO communications,” IEEE Trans. Wireless Commun., 2022, to be published.
- [11] X. Chen, S. Zhang, and Q. Li, “A review of mutual coupling in MIMO systems,” IEEE Access, vol. 6, pp. 24 706–24 719, Apr. 2018.
- [12] J. W. Wallace and M. A. Jensen, “Mutual coupling in MIMO wireless systems: a rigorous network theory analysis,” IEEE Trans. Wireless Commun., vol. 3, no. 4, pp. 1317–1325, Jul. 2004.
- [13] K. Mammasis, R. W. Stewart, and J. S. Thompson, “Spatial fading correlation model using mixtures of von Mises Fisher distributions,” IEEE Trans. Wireless Commun., vol. 8, no. 4, pp. 2046–2055, Apr. 2009.
- [14] 3GPP TR 38.901, “Study on channel model for frequencies from 0.5 to 100 GHz,” 2020.
- [15] K. V. Mardia and P. E. Jupp, Directional Statistics. New York: John Wiley & Sons Ltd, 2000.
- [16] P. Hannan, “The element-gain paradox for a phased-array antenna,” IEEE Trans. Antenna Propag., vol. 12, no. 4, pp. 423–433, Jul. 1964.
- [17] P. Kidal, A. Vosoogh, and S. Maci, “Fundamental directivity limitations of dense array antennas: A numerical study using Hannan´s embedded element efficiency,” IEEE Antenna Wireless Propag. Lett., vol. 15, pp. 766–769, Aug. 2015.
- [18] W. Yu, “Sum-capacity computation for the Gaussian vector broadcast channel via dual decomposition,” IEEE Trans. Inf. Theory, vol. 52, no. 2, pp. 754–759, Feb. 2006.

Thank You